Physics Letters A 381 (2017) 1123–1128

Contents lists available at ScienceDirect

Physics Letters A

www.elsevier.com/locate/pla

Discussion

Long-ranged Fermi–Pasta–Ulam systems in thermal contact: Crossover from q-statistics to Boltzmann–Gibbs statistics

Debarshee Bagchi [a,*], Constantino Tsallis [a,b,c,*]

[a] Centro Brasileiro de Pesquisas Fisicas, Rua Xavier Sigaud 150, 22290-180 Rio de Janeiro, RJ, Brazil
[b] National Institute of Science and Technology of Complex Systems, Rua Xavier Sigaud 150, 22290-180 Rio de Janeiro, RJ, Brazil
[c] Santa Fe Institute, 1399 Hyde Park Road, New Mexico 87501, USA

ARTICLE INFO

Article history:
Received 16 December 2016
Received in revised form 23 January 2017
Accepted 31 January 2017
Available online 7 February 2017
Communicated by C.R. Doering

Keywords:
Relaxation
Fermi–Pasta–Ulam
Long-range interactions
q-statistics

ABSTRACT

The relaxation to equilibrium of two long-range-interacting Fermi–Pasta–Ulam-like models (β type) in thermal contact is numerically studied. These systems, with different sizes and energy densities, are coupled to each other by a few thermal contacts which are short-range harmonic springs. By using the kinetic definition of temperature, we compute the time evolution of temperature and energy density of the two systems. Eventually, for some time $t > t_{eq}$, the temperature and energy density of the coupled system equilibrate to values consistent with standard Boltzmann–Gibbs thermostatistics. The equilibration time t_{eq} depends on the system size N as $t_{eq} \sim N^{\gamma}$ where $\gamma \simeq 1.8$. We compute the velocity distribution $P(v)$ of the oscillators of the two systems during the relaxation process. We find that $P(v)$ is non-Gaussian and is remarkably close to a q-Gaussian distribution for all times before thermal equilibrium is reached. During the relaxation process we observe $q > 1$ while close to $t = t_{eq}$ the value of q converges to unity and $P(v)$ approaches a Gaussian. Thus the relaxation phenomenon in long-ranged systems connected by a thermal contact can be generically described as a crossover from q-statistics to Boltzmann–Gibbs statistics.

1. Introduction

It is well known that gravitation strongly challenges the thermostatistical theory developed by Boltzmann and Gibbs: Gibbs himself pointed this out in his celebrated 1902 book [1]. Since then, a large literature has addressed this type of difficulty, especially in what concerns long-range-interacting systems (see, for instance, [2–16]). In fact, macroscopic physical systems with long-range interactions are ubiquitous in nature, some examples being (in addition to self-gravitating systems) granular matter, biological systems, vortices in superconductors, hot plasma, dipolar ferroelectrics and ferromagnets [11,13]. These systems have induced a flurry of research activities in recent times primarily because of two reasons. Firstly, from the theoretical perspective, it is found that long-ranged systems have very rich, and often peculiar, thermo-statistical properties such as breakdown of ergodicity, ensemble inequivalence, weak chaos, thermodynamical nonextensivity for the total energy, metastable states, negative specific heat, phase transitions even in one dimension – all of which are not always describable in the conventional framework of Boltzmann–Gibbs (BG) statistical mechanics [7,11,12]. Thus one needs to propose new theoretical concepts and principles in order to have a satisfactory understanding of the underlying physics of these systems; one such approach being the non-extensive thermostatistics [12,17]. Secondly, besides the purely theoretical interest, many experimental and computational works [18–33] are also being performed these days on a variety of systems that exhibit one or more of the above-mentioned features and, as such, the theoretical predictions can be tested and verified in controlled laboratory experiments.

In physics, relaxation processes of various kinds are routinely studied; theoretically [34–36] and also in large number of experiments in magnetism, glassy systems, polymers, superconductors, liquid crystals [37] to name a few. This gives us valuable information about the dynamical properties of the system under investigation. For long-range-interacting systems, it is known that the order of the limits $N \to \infty$ and $t \to \infty$ (where N, t are system size and time respectively) is crucial and generally these two limits do not commute [34]. Depending on the order in which the limit is executed, one can have a Gaussian or a non-Gaussian velocity distribution function at late times. Such a problem is not usual for a short-ranged system and so one needs to be more cautious while investigating relaxation processes in many-body systems with long-range interactions.

* Corresponding authors.
E-mail addresses: debarshee@cbpf.br (D. Bagchi), tsallis@cbpf.br (C. Tsallis).

http://dx.doi.org/10.1016/j.physleta.2017.01.057
0375-9601/

In this paper we study theoretically, using extensive numerical simulation, such a relaxation process of two classical nonlinear lattices with long-range interaction and coupled by a thermal contact. This is also partly inspired by recent theoretical works on superconductors [25,38] concerning the over-damped motion of interacting vortices in type-II superconductors within the framework of non-extensive statistical mechanics. In [38] a type-II superconductor with vortices is coupled to a "vortex reservoir" which is a system with a much larger number of vortices and the relaxation process is studied in terms of an effective temperature that depends on the vortex density and interaction among vortices. Pluchino et al. studied relaxation to equilibrium in the Hamiltonian Mean Field (HMF) model with a particular class of initial conditions [39]. Through numerical simulations they observed quasi-stationary states that became stable if the thermodynamic limit is reached faster than the infinite time limit as was mentioned previously [34]. These quasi-stationary states exhibit interesting anomalies such as anomalous diffusion, non-Gaussian velocity distributions, weak chaos, ergodicity breakdown, aging, quite similarly to what is observed in glassy systems. In another work [40], the dynamics of a small long-range interacting system in contact with a large long-range thermal bath, both being HMF models, is studied in terms of the kinetic temperature and various anomalous properties of the relaxation process in the quasi-stationary states were reported. Very recently another work [41] studied chaos properties and relaxation to equilibrium of two coupled HMF models and discovered, quite surprisingly, that weak chaos in some cases favors faster relaxation than strong chaos.

Motivated by these novel ideas and results, we study here a thermal relaxation process of two coupled Fermi–Pasta–Ulam (FPU) oscillator lattices with long-range interactions *via* a thermal contact. Using direct (first principles) integration of the equations of motion of the particles we study the time evolution of this coupled system by studying the time series for energy density and temperature, and by computing velocity distribution of the oscillators. The velocity distribution function provides valuable knowledge about how the underlying physics of such coupled long-range systems evolves with time. The specific questions that we wish to examine are broadly: (a) Is there an equilibration of the two nonlinear long-ranged systems similar to that of ordinary short-ranged systems *via* the thermal contact? (b) Nature of the relaxation process and the final equilibrium state: is the velocity distribution function a Gaussian ($q = 1$) or a non-Gaussian, for instance a q-Gaussian with $q \neq 1$?

In the following we demonstrate that this relaxation process is a crossover from non-extensive statistical mechanics to Boltzmann–Gibbs' statistical mechanics at late times. The remainder of the paper is arranged as follows. In Sec. 2, we describe the notations and formulae involved, the numerical scheme employed and the numerical experiment performed. We present our results in Sec. 3 and conclude with a discussion in Sec. 4.

2. Model and numerical approach

As already mentioned, we numerically investigate the relaxation to equilibrium of two long-ranged (β type) Fermi–Pasta–Ulam systems that are connected to each other by a thermal contact. The thermal contact is a short ranged interaction of the harmonic type. Each of the systems has the Hamiltonian [15]

$$\mathcal{H} = \sum_i \frac{{p_i}^2}{2m_i} + \frac{a}{2}\sum_i (x_{i+1} - x_i)^2 + \frac{b}{4\tilde{N}}\sum_i \sum_{j\neq i} \frac{(x_i - x_j)^4}{d_{ij}^{\alpha}}, \quad (1)$$

where x_i and p_i are the displacement and momentum of the i-th particle with mass m_i (all m_i set to unity); $a \geq 0$, $b > 0$, and $\alpha \geq 0$. Here d_{ij} is the shortest Euclidean distance between the i-th and

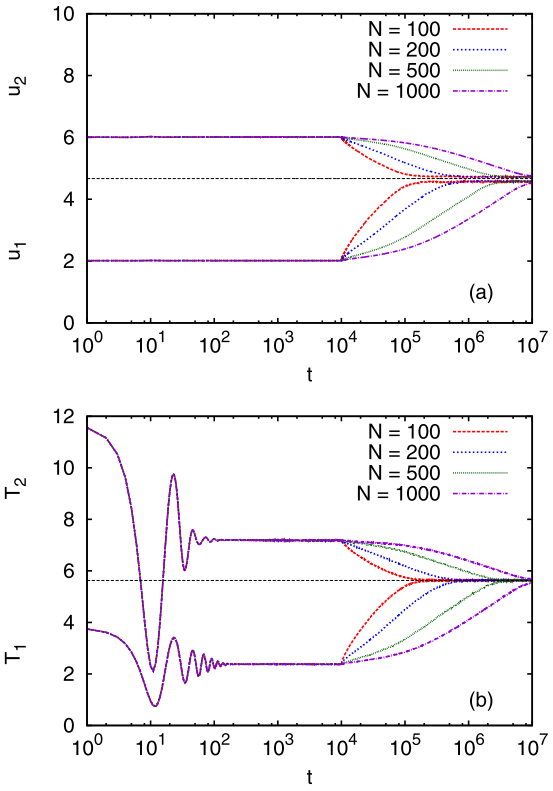

Fig. 1. (Color online.) Time series of (a) energy density and (b) temperature for the two systems for different values of the size N. The system sizes are chosen as $N_1, N_2 = N, rN$ with $r = 2$ here. The parameters used here are $a = b = 1$, $\alpha = 0.9$; energy densities are $u_1 = 2$ and $u_2 = 6$. The thermal contact is connected at $t = t_c = 10^4$. Therefore $k_c = 0$ for $t < t_c$ and $k_c = 1$ for $t > t_c$. The dotted horizontal lines in (a) and (b) represent u_{eq} and T_{eq} respectively (Eqs. (6)). Note that, in (a) the individual energy densities u_1 and u_2 do not converge to u_{eq} but in (b) the individual temperatures T_1 and T_2 do converge to T_{eq} for $t > t_{eq}$, thus implying that the two systems are in thermal equilibrium with each other (see text).

j-th lattice sites ($1 \leq i, j \leq N$); we use periodic boundary conditions. If $\alpha > 1$ ($0 \leq \alpha \leq 1$) we have short-range (long-range) interactions in the sense that the potential energy per particle converges (diverges) as $N \to \infty$; in particular, the limit $\alpha \to \infty$ corresponds to only first-neighbor interactions, and the $\alpha = 0$ value corresponds to typical mean field scenario. The Hamiltonian is made extensive for all values of α by adopting the scaling factor $\tilde{N}$ [15,14]

$$\tilde{N} \equiv \sum_{i=1}^{N} \frac{1}{d_{ij}^{\alpha}}; \quad (2)$$

hence $\tilde{N}$ depends on α, N, and the boundary conditions used. Note that for $\alpha = 0$ we have $\tilde{N} = N$, which recovers the rescaling usually introduced in mean field approaches known as the Kac prescription factor. In the thermodynamic limit, $N \to \infty$, $\tilde{N}$ remains constant for $\alpha > 1$, whereas $\tilde{N} \sim \frac{N^{1-\alpha}}{1-\alpha}$ for $0 \leq \alpha < 1$ ($\tilde{N} \sim \ln N$ for $\alpha = 1$).

In the following, we outline the numerical experiment that we perform and establish the notations and formulae used in the computation. We choose two systems S_1 and S_2 with N_1 and N_2 oscillators respectively. Since the long-range interaction part of the Hamiltonian Eq. (1) depends on the number of oscillators in the system via $\tilde{N}$ Eq. (2), so essentially the two systems have asymmetric interaction strength among the oscillators for $N_1 \neq N_2$. We start from random initial displacements x_i drawn from a uniform

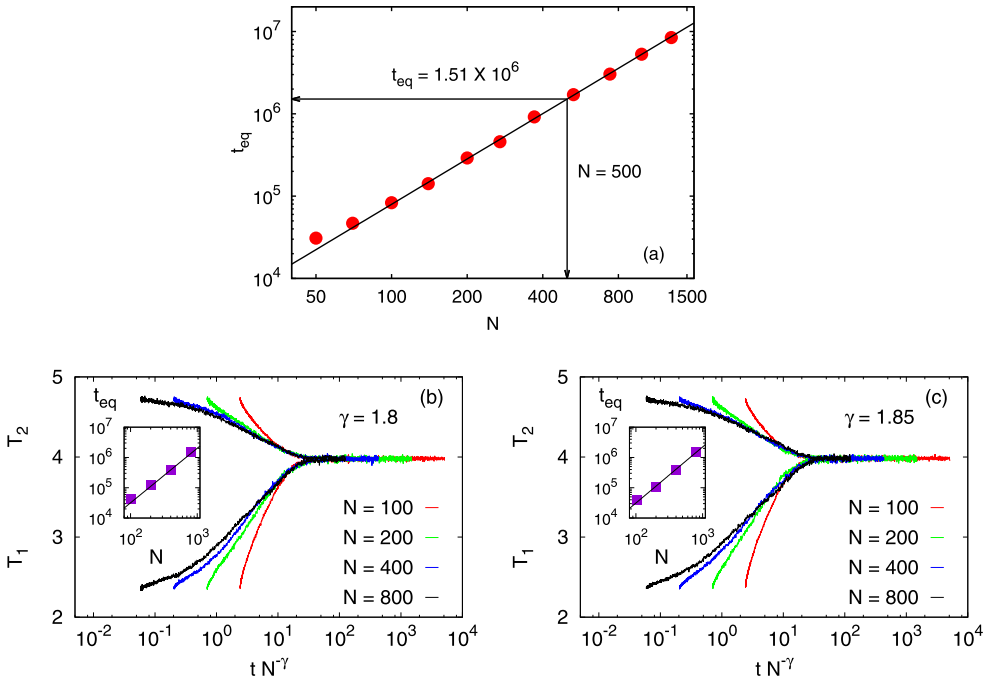

Fig. 2. (Color online.) (a) Log-log plot of the variation of t_{eq} with N. For larger system sizes, $t_{eq} \sim N^{\gamma}$ with $\gamma = 1.8$ for $\alpha = 0.9$ and $(u_1, u_2) = (2, 6)$. We show, for different system size N, the temperature time series as a function of rescaled time t/N^{γ}: (b) for $\alpha = 0.6$ and $(u_1, u_2) = (2, 4)$ we have $\gamma = 1.8$; (c) for $\alpha = 0.9$ and $(u_1, u_2) = (2, 4)$ we have $\gamma = 1.85$; all other parameters remaining the same as in (a).

distribution centered around zero, and momenta p_i from a Gaussian distribution with zero mean and unit variance. The velocities are re-scaled so that the two systems have energy per particle $u_{1,2} = U_{1,2}/N_{1,2}$ (where $U =< \mathcal{H} >$) at time $t = 0$. Thereafter, we evolve the two systems independently without the thermal contact. The time evolution of the systems is numerically performed by integrating the equations of motion (Newton's law) using a symplectic velocity Verlet algorithm with time-step $\Delta t = 0.05$ (for more details of the integration scheme see [16]).

Since the energy density of the systems is set to different values $u_1 \neq u_2$, after the transients, the two systems settle down to distinct steady states with a constant (within statistical accuracy) temperatures T_1 and T_2. The temperature here is the conventional kinetic temperature that one derives from the equipartition of energy i.e., $T = p^2/m$ (the Boltzmann constant k_B is set to unity) for a one dimensional system.

Once such a steady state is reached, we connect these two long-ranged systems via n thermal contacts which are of the harmonic type $\mathcal{H}_c = \frac{1}{2}k_c(x_k - x_l)^2$, where k and l are oscillator indices belonging to the S_1 and S_2 respectively; k_c is the coupling constant which we set to unity without loss of generality, unless specified otherwise. Thus the Hamiltonian for the combined system is expressed as

$$\mathcal{H}_{12} = \mathcal{H}_1 + \sum_n \mathcal{H}_c^{(n)} + \mathcal{H}_2, \tag{3}$$

where, $\mathcal{H}_c^{(n)}$ is the energy function for the n contacts between the two systems $\mathcal{H}_1$ and $\mathcal{H}_2$. If the number of thermal contacts $n << N_1, N_2$, the second term on the right hand side of the above equation is negligibly small compared to the other two terms and hence the coupled system S_{12} will have energy $U_1 + U_2$ approximately. For all our results presented in this paper we choose $n = 2$. Thus two contact sites for each system are chosen arbitrarily and are kept fixed after the contact is established.

Next, we compute the velocity distribution $P(v)$ of the oscillators when the two systems are going through the entire process mentioned above. The velocity distribution at different times is computed by plotting a histogram of the velocities of *all* the oscillators collected over a small time window (typically ~ 50 time-steps) and repeat this for many realizations of the initial conditions (typically $\sim 10^3$) in order to obtain good statistics. From these histograms we can also compute the q-kurtosis κ_q of the distribution which is defined as [14,15,42]

$$\kappa_q = \frac{\int_{-\infty}^{\infty} dv\ v^4 [P(v)]^{2q-1} / \int_{-\infty}^{\infty} dv [P(v)]^{2q-1}}{3\left[\int_{-\infty}^{\infty} dv\ v^2 [P(v)]^{q} / \int_{-\infty}^{\infty} dv [P(v)]^{q}\right]^2}; \tag{4}$$

the value of q is obtained by fitting as we shall show in the next section. Using Eq. (4) the q-kurtosis of any histogram can be computed. It can be verified that $\kappa_q = (3 - q)/(1 + q)$ for any q-Gaussian function velocity distribution

$$G_q(v) = A\left[1 - \beta(1 - q)v^2\right]^{1/(1-q)} \quad (A > 0;\ \beta > 0)\,. \tag{5}$$

Note that, for $q \to 1$, we recover the well known kurtosis $\kappa_1 = \langle x^4 \rangle / 3\langle x^2 \rangle^2 = 1$ corresponding to Gaussian distributions.

3. Simulation results

Let us now present the results of our numerical analysis. We start by fixing the energy densities of the two systems to $(u_1, u_2) = (2, 6)$ and the number of oscillators $(N_1, N_2) = (N, rN)$ where we choose N to be an integer (for our simulations we always choose $N_1 < N_2$ i.e. $r > 1$, and $u_1 < u_2$). All other parameters, apart from the long-range parameter α, of the two systems are set to unity. As is usually the case, all quantities are measured in dimensionless units. We perform the numerical experiment as has been outlined in the previous Sec. 2.

In Fig. 1 we present the time evolution of the energy density and temperature of the two systems for $N = 100, 200, 500, 1000$

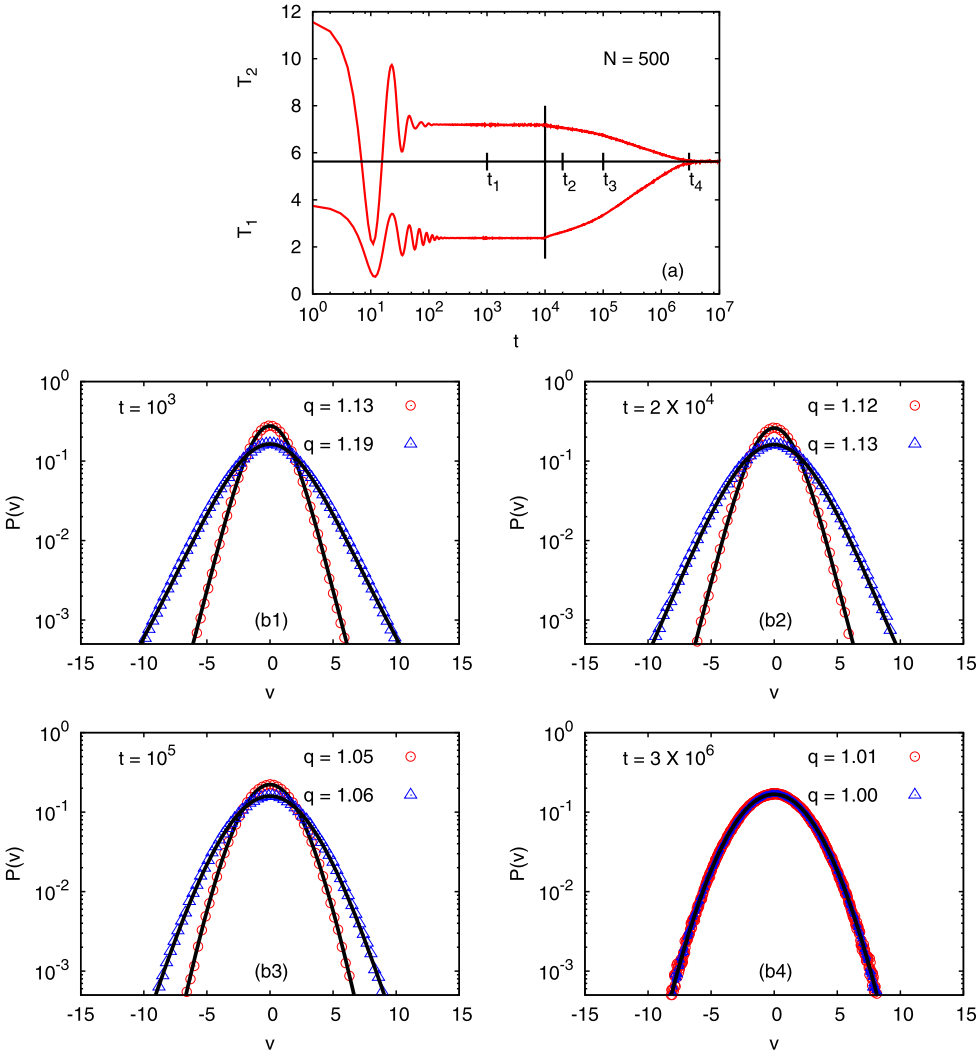

Fig. 3. (Color online.) (a) The time series of temperature T_1, T_2 of the two systems $(N_1, N_2) = (N, rN)$ with $N = 500$. Along the time axis we choose four t values $t = t_1, t_2, t_3$, and t_4 where we compute the velocity distributions of the oscillators in the two systems. The four histograms are shown in (b1)–(b4). We fit the data for the velocity histograms to q-Gaussian distributions (shown by continuous lines) and plot them along with the data from simulation.

with $r = 2$. The energy densities u_1, u_2 remain steady since u is a constant of motion – the systems are micro-canonical ones. At small t, the temperatures (T_1, T_2) oscillate wildly but attain a steady value for $t > 10^2$ in both the systems. Once the stationary temperatures are attained at $t = 10^4$, the two systems are coupled to each other by $n = 2$ thermal contacts. Thereafter both energy density and temperature of the two systems approach each other and at $t = t_{eq}$ equilibrate to a final energy and temperature. Remarkably, we find that the coupled system attains a final energy density and temperature same as that for conventional statistical mechanics namely

$$u_{eq} = \frac{u_1 + ru_2}{1+r} \qquad T_{eq} = \frac{T_1 + rT_2}{1+r}, \tag{6}$$

and therefore independent of the nature of the interaction i.e., the value of α chosen for the two long-ranged FPU systems. Eqs. (6), which are expected in presence of short-range interactions, hold even for our long-range model because of the factor $\tilde{N}$ which makes the long-range system extensive for all values of α. Note that T_1, T_2 in Eq. (6) are the temperatures after the transients have died out $(t > 10^2)$. Since the two systems are asymmetric in their parameters, the individual energy densities do not coincide $(u_1(t) \neq u_2(t)$ for $t > t_{eq}$ as shown in Fig. 1a, or more precisely, $\langle \mathcal{H}_1 \rangle / N_1 \neq \langle \mathcal{H}_2 \rangle / N_2 \neq (\langle \mathcal{H}_1 \rangle + \langle \mathcal{H}_2 \rangle)/(N_1 + N_2) \equiv u_{eq}$ for $t > t_{eq}$, where u_{eq} is defined in Eqs. (6). The individual temperatures however coincide and thermal equilibrium is achieved between the two systems (Fig. 1b).

Note that the relaxation time t_{eq}, at which the two systems have the same temperature, depends on the system size N. Thus the larger the systems, the longer it takes for the coupled system to attain thermal equilibrium. We have estimated the dependence of t_{eq} on N. This is numerically done in the following manner. We scan through the time series of temperature and calculate the difference $|T_1(t) - T_2(t)|$. For $t \geq t_{eq}$ we expect,

$$|T_1(t) - T_2(t)| \leq \epsilon, \tag{7}$$

where $\epsilon \sim N^{-1}$ is a small preset tolerance and the value of t_{eq} is estimated using the equality condition in Eq. (7). The dependence of t_{eq} *vs* N is shown in Fig. 2. From the figure it is seen that $t_{eq} \propto N^{\gamma}$ for large N; the exponent $\gamma \approx 1.8$. We estimated the value of the exponent γ for different values of the parameter α and energy per particle (u_1, u_2). We plot the time series of tem-

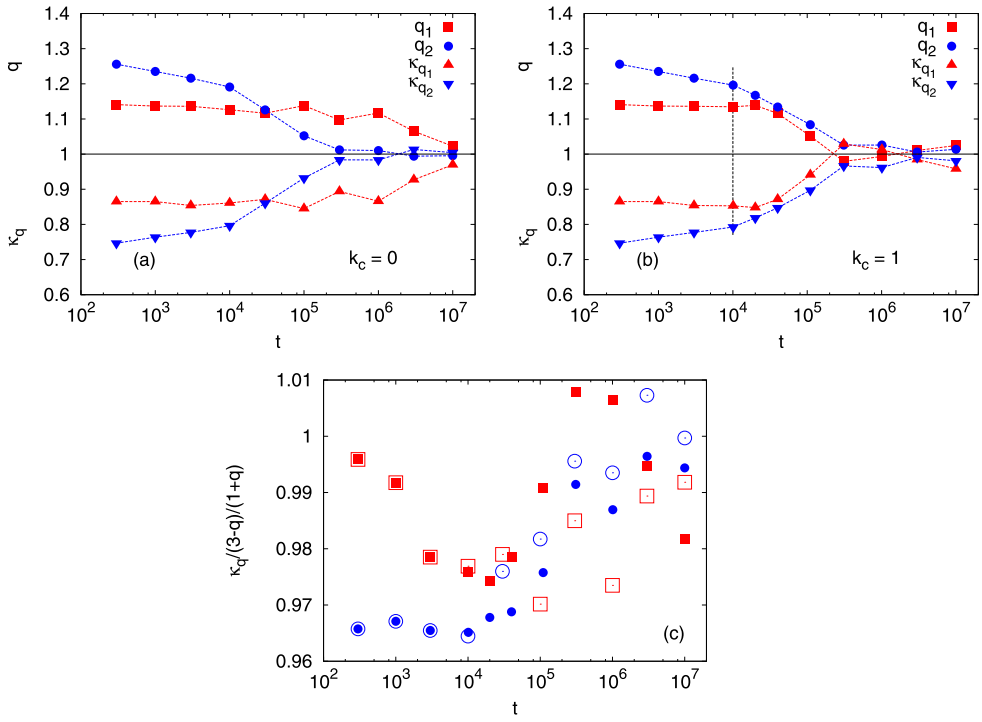

Fig. 4. (Color online.) Plot of the q values (q_1, q_2) and q-kurtosis $(\kappa_{q_1}, \kappa_{q_2})$, as obtained from the velocity histograms of the two systems as a function of time t: (a) without thermal contact $k_c = 0$ and (b) with thermal contact $k_c = 1$. (c) Plot for $\frac{\kappa_q}{(3-q)/(1+q)}$ with time t: square (circle) data-points represent system $S_1(S_2)$, and open (filled) data-points represent $k_c = 0$ ($k_c = 1$) respectively. Here $N = 500$ as in Fig. 3.

peratures (T_1, T_2) with rescaled time $t \to t/N^{\gamma}$ and estimate the value of the exponent γ by the collapse of the time when the two systems have practically the same temperature for all the curves. This is shown in Fig. 2b for $\alpha = 0.6$ and $(u_1, u_2) = (2, 4)$ and in Fig. 2c for $\alpha = 0.9$ and $(u_1, u_2) = (2, 4)$. We find that γ changes nominally with the change of these parameters. We also checked that increasing the number of contacts n, say from $n = 2$ to $n = 10$, the equilibration for fixed N is approached faster, as intuitively expected. Interestingly, the scaling $t_{eq} \sim N^{\gamma}$ still holds and with the same value γ (we obtain $\gamma \approx 1.85$ for $n = 10$ with the other parameters being the same as in Fig. 2c) independent of the value of n. However, we prefer to keep a small value $n << N$, so as to have the total energy of the combined system after contact virtually equal to the sum of their individual energies before contact.

Next, we compute the velocity distribution of the two systems for multiple instances of time before and after the thermal contact is made. We choose $N = 500$ and for this value of N $t_{eq} \approx 1.51 \times 10^6$ as can be seen from Fig. 2. Therefore, from $t = 10^4$ (when the thermal contact is established) to $t \approx 1.51 \times 10^6$ the coupled system is in transition to the final equilibrium state. The normalized velocity distributions are shown above in Fig. 3 for different instants of time. We find that the distribution of velocities is numerically close to a q-Gaussian and is also known from previous studies for the long-ranged FPU model in one dimension [15]. As such we fit the normalized histograms to a q-Gaussian distribution Eq. (5).

In Fig. 3 we have fit the data down to a range where $P(v) \sim 1/N$, the larger N being 10^3 in this case. Remarkably enough, we find that the data fit is quite satisfactory for over two decades of magnitude for both the decoupled and coupled systems. Thus one can see that for small t, $q > 1$ whereas $q \to 1$ as t becomes large. In other words, the velocity distribution is similar to a q-Gaussian at small times and eventually becomes a Gaussian. Note that the velocity distribution is a key signature of the underlying statistics and this is what justifies the title of the present manuscript: indeed, there is a crossover from q-statistics, marked by q-Gaussian velocity distributions, to Boltzmann–Gibbs statistics (with the usual Gaussian velocity distributions) at late times.

We perform this exercise for many time instances and extract the q values from the velocity distributions. Using this q, we also compute the q-kurtosis κ_q using Eq. (4) with the value of q obtained from fitting the velocity histograms to q-Gaussian distribution. These two quantities are shown in Fig. 4 for $N_1, N_2 = 500, 1000$ as a function of time both in absence ($k_c = 0$) and presence ($k_c = 1$) of the thermal contact respectively.

For $k_c = 0$ (Fig. 4a) the q-values for S_1 (filled squares) remain roughly constant till they become $q_1 \approx 1$ at $t > 10^7$ whereas the other system S_2 (filled circles) has a sharper variation and $q_2 \approx 1$ for $t > 10^5$. This is because of the fact that S_2 has a higher temperature (since, $u_1 < u_2$) and therefore has a faster approach to unity as compared to S_1. Note that for two systems at the same temperature, the one with larger size would approach $q = 1$ slower. Thus, the approach to $q = 1$ is an interplay of the system size and the temperature, all other parameters remaining the same.

In presence of thermal contact $k_c = 1$ (Fig. 4b), S_1 also has q values close to unity at $t > 10^5$ similar to S_2. Thus S_2 *forces* S_1 to have $q = 1$ since now the two systems are coupled to each other via the thermal contact. Thus at large times $t > 10^6$ both systems become essentially Boltzmann–Gibbs with $q = 1$ and $\kappa_q = 1$. The effect of the thermal contact therefore is to accelerate the attainment of BG behavior for the two coupled systems.

In order to show that the velocity histograms are indeed numerically close to q-Gaussian distributions, we compare κ_q obtained using Eq. (4) to the analytical value of $(3-q)/(1+q)$ i.e., the expression of κ_q obtained by substituting $P(v)$ in Eq. (4) by $G_q(v)$ from Eq. (5). In Figs. 4a and b, to obtain the value of q and κ_q we have used velocity distribution data up to $P(v) \geq 10^{-5}$. In Fig. 4c we show the ratio the kurtosis values obtained numerically and

theoretically as $\frac{\kappa_q}{(3-q)/(1+q)}$. It is found that the maximum discrepancy with regard to unity is always less than $\sim 4\%$, which indicates that the velocity distribution is well represented by a q-Gaussian.

4. Conclusion

To summarize, we coupled two long-range-interacting Fermi–Pasta–Ulam lattices (under periodic boundary conditions) *via* a short ranged harmonic thermal contact and studied the relaxation process numerically. Before the contact is established the two long-ranged systems exhibit non-Gaussian velocity distributions that fit very well to q-Gaussians. However, as soon as the thermal contact is established both systems start to approach equilibration to a unique final temperature consistent with conventional thermostatistics. The equilibration time t_{eq} is found to increase as a power-law with the number of oscillators in the system; this is also true for short range interactions albeit with a different exponent. We compute the value of q and q-kurtosis from the histograms of velocities. We find that the relaxation to equilibrium happens only if *both* systems satisfy Boltzmann–Gibbs statistical mechanics (hence, $q = 1$ and $\kappa_q = 1$) whereas, for all times before equilibration, the systems possibly satisfy q-statistics (with $q > 1$ and $\kappa_q < 1$). However, if we compare this work with Ref. [38], in the latter the two systems that exchange concentrations of vortices between them without a physical thermal contact of the usual kind (like the present one), maintain their non-Gaussian velocity distributions all the way long, including the final equilibrium states. We speculate that this could be attributed to the manner in which the energy exchange process happens here mediated by the thermal contact. The two systems even for $\alpha < 1$ (in one dimension) no longer remain weakly chaotic (i.e., Lyapunov exponent $\lambda \to 0$ for $N \to \infty$ as a power-law [15,16]) and possibly any hierarchical structure of the phase space is lost – the coupled system becomes well-mixed and exhibits Gaussian velocity distributions. An important question at this point is to address possible coupling mechanisms that preserve the non-Gaussian behavior even at late times when the two long-ranged systems achieve equal kinetic and/or effective temperatures. We intend to explore these aspects in future works.

We acknowledge fruitful discussions with P. Rapcan and G. Sicuro, as well as partial financial support from CNPq and FAPERJ (Brazilian agencies) and the John Templeton Foundation (USA).

References

[1] J.W. Gibbs, Elementary Principles in Statistical Mechanics – Developed with Especial Reference to the Rational Foundation of Thermodynamics, C. Scribner's Sons, New York, 1902; Yale University Press, New Haven, 1948; OX Bow Press, Woodbridge, Connecticut, 1981, p. 35.
[2] M. Antoni, S. Ruffo, Phys. Rev. E 52 (1995) 2361.
[3] V. Latora, A. Rapisarda, S. Ruffo, Phys. Rev. Lett. 80 (1998) 692.
[4] C. Anteneodo, C. Tsallis, Phys. Rev. Lett. 80 (1998) 5313.
[5] T. Dauxois, V. Latora, A. Rapisarda, S. Ruffo, A. Torcini, in: T. Dauxois, S. Ruffo, E. Arimondo, M. Wilkens (Eds.), Lect. Notes Phys., vol. 602, 2002, p. 458.
[6] A. Pluchino, V. Latora, A. Rapisarda, Physica A 340 (2004) 187.
[7] M. Gell-Mann, C. Tsallis (Eds.), Nonextensive Entropy – Interdisciplinary Applications, Oxford University Press, New York, 2004.
[8] A. Pluchino, V. Latora, A. Rapisarda, Physica A 370 (2006) 573.
[9] A. Pluchino, A. Rapisarda, C. Tsallis, Europhys. Lett. 80 (2007) 26002.
[10] A. Pluchino, A. Rapisarda, C. Tsallis, Physica A 387 (2008) 3121.
[11] A. Campa, T. Dauxois, S. Ruffo, Phys. Rep. 480 (2009) 57.
[12] C. Tsallis, Introduction to Nonextensive Statistical Mechanics – Approaching a Complex World, Springer, New York, 2009.
[13] T. Dauxois, S. Ruffo, L.F. Cugliandolo (Eds.), Long-Range Interacting Systems, Oxford University Press, New York, 2010.
[14] L.J.L. Cirto, V.R.V. Assis, C. Tsallis, Physica A 393 (2013) 286.
[15] H. Christodoulidi, C. Tsallis, T. Bountis, Europhys. Lett. 108 (2014) 40006.
[16] D. Bagchi, C. Tsallis, Phys. Rev. E 93 (2016) 062213.
[17] C. Tsallis, J. Stat. Phys. 52 (1988) 479;
C. Tsallis, R.S. Mendes, A.R. Plastino, Physica A 261 (1998) 534.
[18] P. Douglas, S. Bergamini, F. Renzoni, Phys. Rev. Lett. 96 (2006) 110601.
[19] B. Liu, J. Goree, Phys. Rev. Lett. 100 (2008) 055003;
E. Lutz, F. Renzoni, Nat. Phys. 9 (2013) 615.
[20] R.M. Pickup, R. Cywinski, C. Pappas, B. Farago, P. Fouquet, Phys. Rev. Lett. 102 (2009) 097202.
[21] R.G. DeVoe, Phys. Rev. Lett. 102 (2009) 063001.
[22] L.F. Burlaga, A.F. Vinas, N.F. Ness, M.H. Acuna, Astrophys. J. 644 (2006) L83.
[23] G. Livadiotis, D.J. McComas, Astrophys. J. 741 (2011) 88.
[24] A. Upadhyaya, J.-P. Rieu, J.A. Glazier, Y. Sawada, Physica A 293 (2001) 549.
[25] J.S. Andrade Jr., G.F.T. da Silva, A.A. Moreira, F.D. Nobre, E.M.F. Curado, Phys. Rev. Lett. 105 (2010) 260601.
[26] CMS Collaboration, Phys. Rev. Lett. 105 (2010) 022002;
CMS Collaboration, J. High Energy Phys. 8 (2011) 86.
[27] ALICE Collaboration, Phys. Lett. B 693 (2010) 53;
ALICE Collaboration, Phys. Rev. D 86 (2012) 112007.
[28] ATLAS Collaboration, New J. Phys. 13 (2011) 053033.
[29] PHENIX Collaboration, Phys. Rev. D 83 (2011) 052004;
PHENIX Collaboration, Phys. Rev. C 84 (2011) 044902.
[30] C.Y. Wong, G. Wilk, Phys. Rev. D 87 (2013) 114007.
[31] L. Marques, E. Andrade-II, A. Deppman, Phys. Rev. D 87 (2013) 114022.
[32] G. Combe, V. Richefeu, M. Stasiak, A.P.F. Atman, Phys. Rev. Lett. 115 (2015) 238301.
[33] S.G.A. Brito, L.R. da Silva, C. Tsallis, Sci. Rep. 6 (2016) 27992.
[34] V. Latora, A. Rapisarda, C. Tsallis, Phys. Rev. E 64 (2001) 056134.
[35] A. Patelli, S. Gupta, C. Nardini, S. Ruffo, Phys. Rev. E 85 (2012) 021133.
[36] C. Tsallis, Physica A 221 (1995) 277–290.
[37] W. Haase, S. Wrobel (Eds.), Relaxation Phenomena, Springer-Verlag, Berlin, Heidelberg, Germany, 2003.
[38] E.M.F. Curado, A.M.C. Souza, F.D. Nobre, R.F.S. Andrade, Phys. Rev. E 89 (2014) 022117.
[39] A. Pluchino, V. Latora, A. Rapisarda, Contin. Mech. Thermodyn. 16 (2004) 245.
[40] P. Buyl, G. Ninno, D. Fanelli, C. Nardini, A. Patelli, F. Piazza, Y. Yamaguchi, Phys. Rev. E 87 (2013) 042110.
[41] F.L. Antunes, F.P.C. Benetti, R. Pakter, Y. Levin, Phys. Rev. E 92 (2015) 052123.
[42] C. Tsallis, A.R. Plastino, R.F. Alvarez-Estrada, J. Math. Phys. 50 (2009) 043303.